Maize *Dek37* Encodes a P-type PPR Protein That Affects *cis*-Splicing of Mitochondrial *nad2* Intron 1 and Seed Development

Dawei Dai,* Shengchao Luan,* Xiuzu Chen,* Qun Wang,* Yang Feng,† Chenguang Zhu,* Weiwei Qi,* and Rentao Song*,†,1

*Shanghai Key Laboratory of Bio-Energy Crops, School of Life Sciences, Shanghai University, 200444, China and †National Maize Improvement Center of China, China Agricultural University, Beijing 100193, China

ABSTRACT Mitochondrial group II introns require the participation of numerous nucleus-encoded general and specific factors to achieve efficient splicing in *vivo*. Pentatricopeptide repeat (PPR) proteins have been implicated in assisting group II intron splicing. Here, we identified and characterized a new maize seed mutant, *defective kernel 37* (*dek37*), which has significantly delayed endosperm and embryo development. *Dek37* encodes a classic P-type PPR protein that targets mitochondria. The *dek37* mutation causes no detectable DEK37 protein in mutant seeds. Mitochondrial transcripts analysis indicated that *dek37* mutation decreases splicing efficiency of mitochondrial *nad2* intron 1, leading to reduced assembly and NADH dehydrogenase activity of complex I. Transmission Electron Microscopy (TEM) revealed severe morphological defects of mitochondria in *dek37*. Transcriptome analysis of *dek37* endosperm indicated enhanced expression in the alternative respiratory pathway and extensive differentially expressed genes related to mitochondrial function. These results indicated that *Dek37* is involved in *cis*-splicing of mitochondrial *nad2* intron 1 and is required for complex I assembly, mitochondrial function, and seed development in maize.

KEYWORDS *Zea mays*; *Dek37*; pentatricopeptide repeat protein; mitochondria; splicing; seed development

PLANT mitochondrial genomes contain 50–60 genes that encode various subunits of multiprotein complexes of respiratory electron transport chain, subunits involved in biogenesis of cytochrome c, transfer RNAs (tRNAs), ribosomal RNAs (rRNAs), and ribosomal proteins (Unseld *et al.* 1997; Kubo *et al.* 2000; Notsu *et al.* 2002; Handa 2003). In maize, the mitochondrial genome encodes 58 genes including 3 ribosomal RNAs, 21 tRNAs that recognize 14 amino acids and 33 known proteins that include 22 proteins for respiratory chain function (18 subunits of complex I, III, IV, and V, 4 subunits involved in cytochrome c biogenesis), 9 ribosomal proteins (RP), a transporter protein (MttB), and a maturase (MatR) (Clifton *et al.* 2004). Recently, the pentatricopeptide repeat (PPR) protein family, a family of RNA-binding proteins involved in many post-transcriptional aspects of plant organellar gene expression, has come into focus (Delannoy *et al.* 2007). PPR proteins are characterized by the presence of tandem arrays of a degenerate 35-amino-acid (pentatricopeptide) motif (Small and Peeters 2000). In both rice and *Arabidopsis* genome sequences, >450 PPR proteins have been annotated (Aubourg *et al.* 2000; Lurin *et al.* 2004). It has been demonstrated that PPR proteins play important roles in various steps in organellar gene expression, including RNA splicing (Schmitz-Linneweber *et al.* 2006; de Longevialle *et al.* 2007; Beick *et al.* 2008; Cohen *et al.* 2014; Colas des Francs-Small *et al.* 2014; Hsieh *et al.* 2015; Xiu *et al.* 2016; Chen *et al.* 2017; Qi *et al.* 2017b), RNA editing (Kotera *et al.* 2005; Liu *et al.* 2013; Sun *et al.* 2015; Qi *et al.* 2017a), RNA cleavage (Hashimoto *et al.* 2003), and translation (Coffin *et al.* 1997; Fisk *et al.* 1999) by genetic approaches. However, the molecular roles and regulatory functions are still unknown for a great number of PPR proteins.

The mitochondrial NADH-ubiquinone reductase (complex I), which is located in the inner membrane, is the major entry point for the electron transport chain in plant and animal mitochondria (Brandt 2006; Noctor *et al.* 2007; Schertl and Braun 2014). This enzyme catalyses the first step in the respiratory chain, the oxidation of NADH and transfer of

doi: https://doi.org/10.1534/genetics.117.300602
Manuscript received December 7, 2017; accepted for publication January 2, 2018; published Early Online January 4, 2018.
Supplemental material is available online at www.genetics.org/lookup/suppl/doi:10.1534/genetics.117.300602/-/DC1.
[1]Corresponding author: Shanghai Key Laboratory of Bio-Energy Crops, School of Life Sciences, Shanghai University, 333 Nanchen Rd., Shanghai 200444, China. E-mail: rentaosong@cau.edu.cn

electrons to ubiquinone. Complex I dysfunction causes reorganization of cellular respiration and affects metabolic processes in mitochondria, plastids, peroxisomes, and other cellular compartments with drastic consequences for growth and development (Fromm *et al.* 2016). The mitochondrial complex I has a molecular mass of ∼1000 kDa and includes 40–50 subunits in animals, fungi, and plants (Heazlewood *et al.* 2003). Based on organelle and nuclear genome sequencing, the majority of these subunits are nuclear encoded since only nine genes have been identified in higher plant complete mitochondrial genomes, which are *nad1*, *nad2*, *nad3*, *nad4*, *nad4L*, *nad5*, *nad6*, *nad7*, and *nad9* (Chomyn *et al.* 1986; Sugiyama *et al.* 2005). More recently, 47 subunits of complex I have been detected by mitochondrial complexome in *Arabidopsis* (Senkler *et al.* 2017). This offers better understanding of previously characterized protein complexes and several unknown protein complexes.

All plant mitochondrial introns belong to the highly structured ribozymic group II class and the majority are located within NADH dehydrogenase (*nad*) genes, which encode complex I components of the respiratory chain (Li-Pook-Than and Bonen 2006). Among various flowering plants, a total of 25 introns have been identified, and that include six *trans*-splicing types (Bonen and Vogel 2001). Only *nad1*, *nad2*, and *nad5* transcripts were identified to require *trans*-splicing among all the mitochondrial transcripts (Malek and Knoop 1998). Much more has been known about the RNA splicing process in chloroplasts and mitochondria (Till *et al.* 2001; Ostheimer *et al.* 2005, 2006; Schmitz-Linneweber *et al.* 2006; de Longevialle *et al.* 2007; Xiu *et al.* 2016; Cai *et al.* 2017; Chen *et al.* 2017; Qi *et al.* 2017b). These studies have indicated that PPR proteins play important roles in mitochondrial RNA splicing processes and in maintaining normal mitochondrial function and activity.

The work reported here characterized a maize seed mutant *dek37* corresponding to a *defective kernel* phenotype. *Dek37* encodes a classic P-type PPR protein that targets mitochondria. *Dek37* is involved in *cis*-splicing of mitochondrial *nad2* intron 1 in developing seeds. Disruption of *Dek37* function results in the reduction of mitochondrial complex I assembly and NADH dehydrogenase activity, as well as impaired mitochondrial function and delayed seed development.

Materials and Methods

Plant materials

The *MuDR* stock (330I) and UFMu05702 mutant lines were obtained from Maize Genetics Cooperation Stock Center. The *MuDR* stock (330I) was crossed into B73 inbred line as male parent to generate F1 population seeds, and then self-crossed to generate the F2 population ears. Phenotypical screening for seed mutants was carried out on F2 ears. The *dek37*-ref and dek37-mu were recovered as *dek* mutants from F2 ear screening, with progenies exhibiting 1:3 segregation of *dek* and wild-type (WT) seed phenotype.

The mature seeds were used for genomic DNA extraction. The immature seeds were harvested for RNA and protein extraction, mitochondria isolation, and paraffin and resin section preparation, as well as TEM observation and RNA-seq. Other plant tissues were harvested from one inbred B73 plant for RNA and protein extraction. The seedlings of B73 inbred line were harvested for chloroplasts preparation at 15 days after germination (DAG). All plants were cultivated in the experimental field in Shanghai University, Shanghai.

Measurements of protein and starch

For the protein measurements, the endosperm of WT and *dek37* mature seeds was separated from the embryo and pericarp by dissection after soaking the seeds in water. The samples were dried to constant weights, pulverized with a mortar and pestle in liquid N2, and then measured according to a previously described protocol (Qi *et al.* 2016). All the measurements were replicated at least three times.

For the starch measurements, five mature seeds of the WT and *dek37* were ground in liquid N2. The resulting powders were dried to a constant weight. Finally, the total starch was measured by using an amyloglucosidase/α-amylase starch assay kit (Megazyme). The method referenced a previously described protocol (Qi *et al.* 2016). All the measurements were replicated at least three times.

Light microscopy, TEM

For light microscopy analysis, immature WT and *dek37* seeds at 12 days after pollination (DAP) and 18 DAP were collected from the same ear and were cut along the longitudinal axis for paraffin section preparation. The sections were fixed in a formalin–acetic acid–alcohol mixture and were dehydrated in an ethanol gradient series of 50, 60, 70, 85, 95, and 100% ethanol. After replacement of acetone and infiltration with paraffin, the sections were embedded and cut using RM2265 (Leica). The paraffin section was stained by fuchsin basic. The sections were observed using Leica DFC500 at Shanghai University.

For TEM analysis, immature WT and *dek37*-ref seeds at 18 DAP were collected from the same ear and were cut along the horizontal axis into small pieces and fixed in paraformaldehyde. The samples were further processed and stained by osmic acid and observed at Shanghai Normal University using "FEI Tecnai Spirit G2 BioTWIN."

Mu tag isolation

The *Mu* tag isolation was performed according to Williams-Carrier *et al.* (2010), with some modifications. Genomic DNA was prepared for mechanical shearing at Majorbio Bio-Pharm Technology (Shanghai, China). Fragments of 200–500 bp were ligated to modified Illumina adapters to mark samples from different individuals. *Mu*-containing DNA fragments were enriched by hybridization to a biotinylated oligonucleotide corresponding to the end of the Mu terminal inverted repeat. Two successive hybrid enrichment steps were performed to ensure that the majority of the sequenced DNA

fragments harbor *Mu* sequences. Using primers that bind to the ends of the adapters, 15 and 18 cycles PCR was used to bulk up the recovered DNA after the first and second selection rounds, respectively. PCR products were cloned into pMD18-T (Takara). Effectiveness of the enrichment was tested by calculating the percentage of clones with *Mu* fragment. Enrichment rate that was above 30% was selected for further *Mu* Illumina sequencing at BerryGenomics (Beijing, China).

RNA extraction and quantitative RT- PCR

Total RNA was extracted with TRIzol reagent (Tiangen) according to a previous study (Feng *et al.* 2009), and DNA was removed by treatment with RNase-Free DNase I (Takara). Using ReverTra Ace reverse transcriptase (Toyobo), RNA was reverse transcribed to complementary DNA using the attached random primers. Amplification of mitochondrial transcripts was performed using primers as described previously (Chen *et al.* 2017).

Quantitative RT-PCR was performed to three independent RNA samples sets with ubiquitin as the reference gene. Quantitative RT-PCR primers of mitochondrial introns were designed as described previously with some modifications (Qi *et al.* 2017b) (Supplemental Material, Table S2 in File S1). Quantitative RT-PCR was performed with SYBR Green Real-Time PCR Master Mix (Toyobo) using a Mastercycler ep realplex 2 (Eppendorf) according to the standard protocol.

Subcellular localization of DEK37

The DNA sequence of full-length DEK37 protein without the stop codon was cloned into pSAT6-EYFP-N1 (vector data are available at http://www.arabidopsis.org/index.jsp). The recombinant plasmid was extracted with ~1 μg total amount and then was introduced into tobacco leaf epidermal cells through transient transformation using the Bio-Rad PDS-1000/HeTM biolistic particle delivery system. The fluorescence signals were detected using LSM710 (Occult International).

Polyclonal antibodies

For antibody production, the DNA sequence corresponding to the 488–765 amino acids of DEK37 was cloned into pET-28a expression vector (Amersham Biosciences). Protein expression was followed by standard procedures. Protein purification and production of antibodies in rabbits were performed according to standard protocols of Abclonal of China. For production of polyclonal antibody against NAD1 (mitochondrial marker, subunit of complex I), the C-terminal 198–214 amino acids were synthesized. Peptide synthesis, peptide purification, and production of antibodies in rabbits were performed according to standard protocols of Abclonal of China. The antibodies against CytC (cytochrome c), COX2 (subunit of complex IV), and D2 (chloroplastic marker) were obtained from Agrisera. The antibody against α-tubulin was obtained from Sigma-Aldrich (St. Louis, MO).

Preparation of mitochondria and chloroplasts

Mitochondria were extracted from inbred B73 immature seeds at 18 DAP as described previously with some modifications (Chen *et al.* 2017). About 15 g of immature seeds at 18 DAP was harvested and ground in liquid nitrogen with a mortar and pestle into powder. Then 20 ml 4° precooled extraction buffer [100 mM tricine, 300 mM sucrose, 10 mM KCl, 1 mM $MgCl_2$, 1 mM EDTA-K, 0.1% BSA, 5 mM DTT (pH 7.4)] and 60 μl of plant protease inhibitor cocktail (Sigma-Aldrich) were added to the ground tissue. All the following steps were performed at 4°. The samples were centrifuged twice at 2600 × *g* for 15 min after filtration through a Miracloth membrane (Calbiochem, San Diego, CA); the supernatant was then centrifuged at 12,000 × *g* for 25 min to pellet the crude mitochondria. The pellet was resuspended in wash buffer [100 mM tricine, 300 mM sucrose, 10 mM KCl, 1 mM $MgCl_2$, 1 mM EDTA-K, 0.1% BSA (pH 7.4)] and loaded on sucrose density gradients of 1.5, 2.5, 2.5, 2, and 2 ml containing 1.8, 1.45, 1.2, 0.9, and 0.6 M sucrose diluted in wash buffer, respectively, according to the protocol described before (Clayton and Shadel 2014), with some modifications. After 90 min of centrifugation at 24,000 rpm at 4°, the mitochondria were collected from the 1.2 M/1.45 M interface and washed four times in wash buffer. The purified mitochondria were collected after 20 min of centrifugation at 12,000 rpm at 4°. Chloroplasts were isolated from B73 inbred line 15 DAG young leaves as described before (Uyttewaal *et al.* 2008).

Immunoblot analysis

Total proteins were extracted from various tissues and organelles, including silk, tassel, ear, root, husk, stem, leaf, and seed. Proteins extracted from developing WT and *dek37* seeds were separated by SDS-PAGE. Separated protein samples were then transferred to a nitrocellulose membrane (0.45 μm; Millipore, Bedford, MA). The membrane with the protein sample attached was incubated with primary and secondary antibodies. Using the SuperSignal West Pico Chemiluminescent Substrate kit (Pierce), the signal was visualized according to the manufacturer's instructions. The polyclonal antibodies against DEK37 and NAD1 were used at 1:500. The antibody against COX2 (Agrisera) was used at 1:1000. The antibodies against CytC (Agrisera), D2 (Agrisera), and α-tubulin (Sigma-Aldrich) were used at 1:5000.

BN-PAGE and NADH dehydrogenase activity examination

The isolated mitochondria were resuspended in 50 μl B25G20 solution (25 mM Bis-Tris, 20% glycerin, pH 7.0), adding 20% DDM to a final concentration of 1% DDM, and were gently mixed on ice for 1.5 hr. After 15 min of centrifugation at 13,000 rpm at 4°, the supernatant was collected and was added to the loading buffer for blue native polyacrylamide electrophoresis. The concentration of the separation gel was from 5 to 13.5%. At first electrophoresis was run at 50 V, and

25 V was added every 20 min to the final 150 V until the loading dye migrated to the edge of the gel. The gel was stained by coomassie brilliant blue. Measurement of NADH dehydrogenase activity was performed as described previously (Meyer *et al.* 2009). Briefly, the gel was washed three times for 5 min with distilled water and incubated in the reaction medium (0.14 mM NADH, 1.22 mM NBT, and 0.1 M Tris-HCl, pH 7.4). When the dark blue stain was strong enough, the reaction was stopped by transferring the gel to 40% methanol/10% acetic acid (v/v).

RNA-seq analysis

Total RNA was extracted from the developing WT and *dek37* seeds at 18 DAP. Library construction was performed according to Illumina standard instructions. Reads were aligned to the maize B73 genome using TopHat2 (Langmead *et al.* 2009). Data were normalized as reads per kilobase of exon per million fragments mapped, as the sensitivity of RNA-seq depends on the transcript length. Significant differentially expressed genes (DEGs) were identified as those with a fold change and *P* value of differential expression above the threshold (fold change >2.0, $P < 0.01$).

Data availability

RNA-seq data are available from the National Center for Biotechnology Information Gene Expression Omnibus (http://www.ncbi.nlm.nih.gov/geo) under the series entry GSE95769. Sequence data from this article can be found in the GenBank/EMBL data libraries under the following accession numbers: *Dek37*, ONM17137, *GRMZM2G021319*; *nad2*, ABE98770.

Results

The dek37 mutation produces small seeds with delayed development

The maize *dek37* is a *defective kernel* (*dek*) mutant isolated from F2 populations containing active *MuDR* (see *Materials and Methods*). The F2 ear that displayed a 1:3 segregation of *dek* and WT seed phenotype was named as *dek37*. The *dek37* mutant seeds are easily distinguished as white and smaller than WT during seed development (18 DAP) (Figure 1A). At maturity, mutant seeds are misshapen (Figure 1, B and C). The 100-seed weight of mutant seeds is only 18% that of the WT (Figure 1G). We analyzed the total starch content and the result showed that the amount of total starch decreased 5% per weight in *dek37* mutant endosperm (Figure 1H). Meanwhile, total storage protein content per weight of mature endosperm was lower in mutant seeds (Figure S1, A and B in File S1).

Detailed phenotypic analyses of WT and *dek37* mutant seeds at different developmental stages showed that development of both the embryo and endosperm is delayed. Longitudinal sections of the whole seed indicated developmental delay in *dek37* compared with the WT (Figure 1D). The endosperm cells of *dek37* seeds at 15 and 18 DAPs were less cytoplasmic dense with fewer starch granules compared with the WT (Figure 1E).

Basal endosperm transfer layer (BETL) cells are critical for nutrient trafficking from the maternal tissue into the developing seeds. To examine the impact of *dek37* mutation on the BETL, we observed the BETL cells at 12, 15, and 18 DAP. The results showed developmental delay of BETL cells in *dek37* seeds as compared with the WT (Figure 1F and Figure S1C in File S1).

The *dek37* mutant seeds showed a low level of germination rate (17%) (Figure 1I). At seedling stage, seedlings of *dek37* displayed developmental delay compared with the WT at 7 DAG (Figure S1D in File S1), and its height was only 50% of the WT (Figure 1J). However, *dek37* seedlings will not survive after emergence of the second leaf. All these results indicated that the *dek37* mutant is homozygous seedling-lethal and the development of *dek37* seeds is significantly delayed compared with the WT.

Cloning of Dek37 gene

Genetic mapping of *Dek37* was carried out with the F2 mapping population. After characterizing 164 individuals, *Dek37* was mapped between the simple sequence repeat (SSR) markers SSR-41 (41,732,004 bp) and SSR-51 (51,098,478 bp), a region encompassing a physical distance of 9 Mb (Figure 2A).

Considering the *dek37*-ref mutant was identified from an active *Mutator* line, *Mu* tags were isolated and sequenced (Williams-Carrier *et al.* 2010). An insertion of a *Mu* element in a PPR gene *GRMZM2G021319* was identified within our mapping interval. The *Mu* insertion is located 5 bp downstream of the start codon. Thus, *GRMZM2G021319* was considered as the candidate gene (Figure 2A).

To confirm if the mutation in *GRMZM2G021319* is the cause for *dek37*, an allelism test was carried out with additional mutant alleles. A *UniformMu* mutant stock (UFMu05702) carrying a *Mu* insertion at 91 bp (*dek37*-mu2) downstream of the start codon in *GRMZM2G021319* was obtained from Maize Genetic Stock Center (Figure 2B). Another allelic mutant (BJ14-32) was identified from our own *Mutator* lines, carrying a *Mu* insertion at 8 bp (*dek37*-mu) downstream of the start codon in *GRMZM2G021319*. An allelism test between *dek37*-ref and *dek37*-mu revealed a 1:3 segregation of *dek* and WT seed phenotype, with 78 *dek* (*dek37*-ref/*dek37*-mu) and 255 WT seeds (Figure 2C). The result indicated that *dek37*-mu cannot complement *dek37*-ref. Therefore, *GRMZM2G021319* is indeed the *Dek37* gene.

Dek37 encodes a P-type PPR protein

Sequence analysis of *Dek37* indicated that it contains a single exon with a 1644 bp open reading frame, which encodes a putative pentatricopeptide repeat protein (Figure 2B). DEK37 was classified as a P-type PPR protein with 10 P repeat domains based on annotation of rice orthologs in FlagDB data (Figure 2B). No E, E+, or DYW domain was found at the C-terminus of DEK37, indicating that DEK37 is a P-type PPR protein (http://urgv.evry.inra.fr/projects/FLAGdb++/HTML/index.shtml).

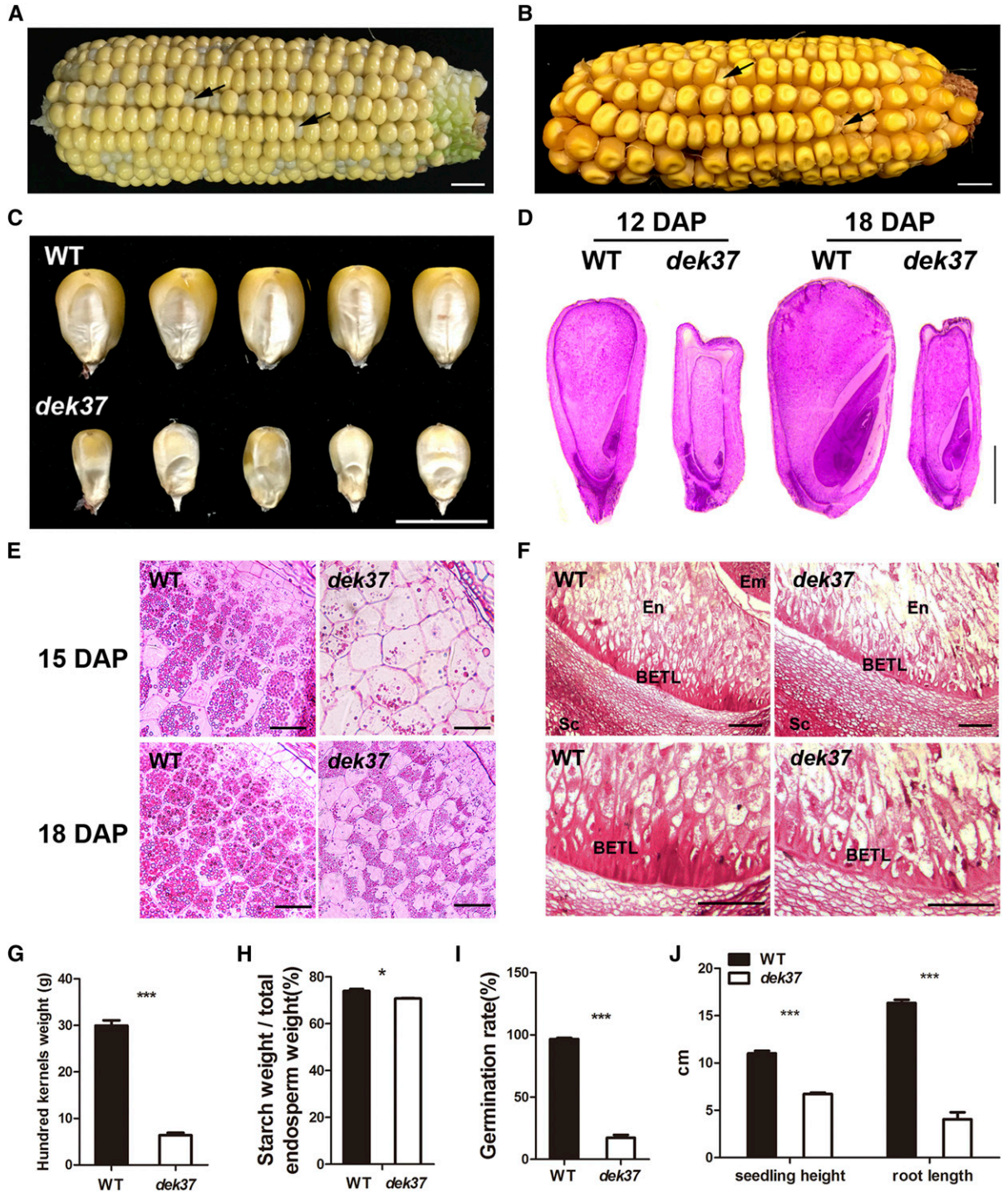

Figure 1 Phenotypic features of maize *dek37* mutant. (A) A 18 DAP F2 ear of *dek37*/WT. The arrows identify two randomly selected mutant seeds. Bar, 1 cm. (B) A mature F2 ear of *dek37*/WT. The arrows identify two randomly selected mutant seeds. Bar, 1 cm. (C) Randomly selected mature WT and *dek37* seeds from segregated F2 population, Bar, 1 cm. (D) Paraffin sections of WT and *dek37* seeds at 12 and 18 DAP. Bar, 1 mm. (E) Microstructure of developing endosperms of WT and *dek37* at 15 and 18 DAP. Bar, 100 μm. (F) BETL cells on paraffin sections of WT and *dek37* at 18 DAP. En, endosperm; Em, embryo; Sc, seed coat. Bar, 50 μm. (G) Comparison of 100-seed weight of randomly selected mature WT and *dek37* seeds in segregated F2 population. Values are the means with SE; $n = 3$ individuals (*** $P < 0.001$, Student's *t*-test). (H) Comparison of total starch content in WT and *dek37* mature endosperm. The measurements were done on per milligram of dried endosperm. Values are the means with SE; $n = 3$ individuals (* $P < 0.05$, Student's *t*-test). (I) Comparison of germination rate of WT and *dek37* mature seeds. Values are the means with SE; $n = 3$ individuals (*** $P < 0.001$, Student's *t*-test). (J) Comparison of seedling height and root length of WT and *dek37*. Values are the means with SE; $n = 20$ seedlings per genotype (*** $P < 0.001$, Student's *t*-test).

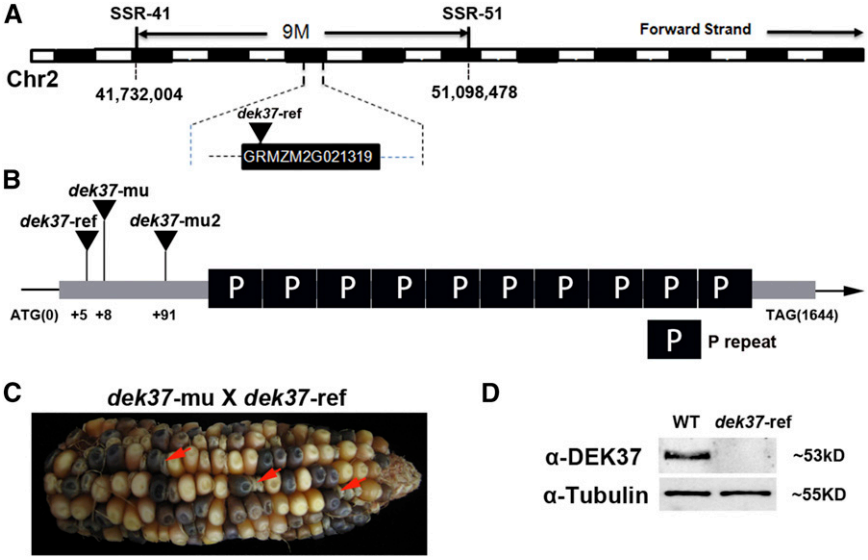

Figure 2 Cloning and identification of *Dek37*. (A) The *Dek37* locus was mapped to an interval of ~9 Mb on chromosome 2. The triangle identifies the site of the *Mu* insertion in the *dek37*-ref mutant. (B) Schematic structure of *GRMZM2G021319* and three allele mutants. The triangles identify the sites of *Mu* insertions. (C) Heterozygous *dek37*-ref and *dek37*-mu were used in an allelism test. The arrows identify three randomly selected *dek* (*dek37*-ref/*dek37*-mu) seeds. (D) Western blot analysis of DEK37 expression in total seed protein from WT and *dek37*-ref immature seeds at 18 DAP. α-tubulin was used as a sample loading control.

To examine mRNA expression of *Dek37*, quantitative RT-PCR was performed with total RNA extracted from 15 to 18 DAP WT and *dek37* immature seeds. Ubiquitin was used as an internal control. Surprisingly, mRNA expression of *Dek37* was significantly up-regulated in *dek37* seeds (Figure S2 in File S1).

To further investigate the expression of DEK37 protein, immunoblot analysis was carried out with DEK37-specific antibody for proteins extracted from WT and *dek37* seeds at 18 DAP. The α-tubulin was used as a loading control. The result showed no detectable DEK37 protein in *dek37* seeds (Figure 2D and Figure S3 in File S1). Therefore, the loss of function of *dek37* is due to the absence of DEK37.

Dek37 is constitutively expressed in various tissues

A phylogenetic tree was constructed based on full-length DEK37 protein and its homologs. The results suggested that DEK37 homologs are highly conserved in angiosperms (Figure 3A). DEK37 is most closely related to Sb06g017980 from *Sorghum bicolor* and Os04g36840 from *Oryza sativa*. A detailed sequence alignment with sorghum, rice, and *Arabidopsis* indicated that DEK37 protein shared highly conserved P repeat domains in monocotyledons (Figure S4 in File S1).

Quantitative RT-PCR analysis revealed that *Dek37* was constitutively expressed in all tested maize tissues, including silk, tassel, ear, root, husk, stem, leaf, and seed (Figure 3B). Expression in the ear was higher than in other tissues. During seed development, *Dek37* was expressed before 3 DAP, and its expression continued later than 30 DAP, with a peak level at 9 DAP (Figure 3B).

DEK37 is localized in mitochondria

Most PPRs are targeted to either plastids or mitochondria, some are dual-localized in both organelles, whereas a few are targeted to nuclei (Lurin *et al.* 2004; Colcombet *et al.* 2013). DEK37 was predicted to have a putative mitochondrial localization signal at the N-terminus based on TargetP analysis (http://www.cbs.dtu.dk/services/TargetP). To experimentally localize DEK37 inside the cell, the full-length DEK37 protein was fused to YFP and transiently expressed in tobacco leaf epidermal cells. Confocal laser scanning microscopy observation revealed that the YFP signal colocalizes with the mitochondria-mCherry marker pBIN20-MT-RK (Nelson *et al.* 2007), indicating that DEK37 is targeted to mitochondria (Figure 3D).

To further validate the mitochondrial localization of DEK37, the subcellular distribution of DEK37 was further analyzed by subcellular fractionation. The intact mitochondria (Figure S5 in File S1) and chloroplasts were isolated, and their protein extracts were collected for western blot analysis. The antibodies against NAD1 [NAD(P)H dehydrogenases 1] (Figure S3 in File S1) and D2 (photosystem II protein) were used as indicators of mitochondrial and chloroplastic fractions, respectively. DEK37 was detected only in the mitochondrial fraction (Figure 3C). These results indicated that DEK37 is localized in mitochondria.

Dek37 participates in cis-splicing of mitochondrial nad2 intron 1

P-type PPR proteins are likely dedicated to RNA stabilization, cleavage, translational activation, splicing, and other RNA processes. DEK37 is a mitochondrion-targeting P-type PPR protein. To gain a general view of changes in mitochondrial transcripts in *dek37* seeds, all mitochondrial protein-encoding genes of WT and *dek37* were analyzed by RT-PCR in WT and *dek37* immature seeds at 18 DAP (Figure 4A and Figure S6 in File S1). The primers anchored to the 5′-UTR and 3′-UTR (near the ATG and stop codon) of every gene were designed to test the full-length coding region (Table S2 in File S1). Most of the mitochondrial genes show indistinguishable expressions between WT and *dek37*, while there was a decreased *nad2* mature transcript in mutant samples (Figure 4A and Figure S6 in File S1). This suggested that *Dek37* is involved in the expression of *nad2* in developing maize seeds. In addition, the

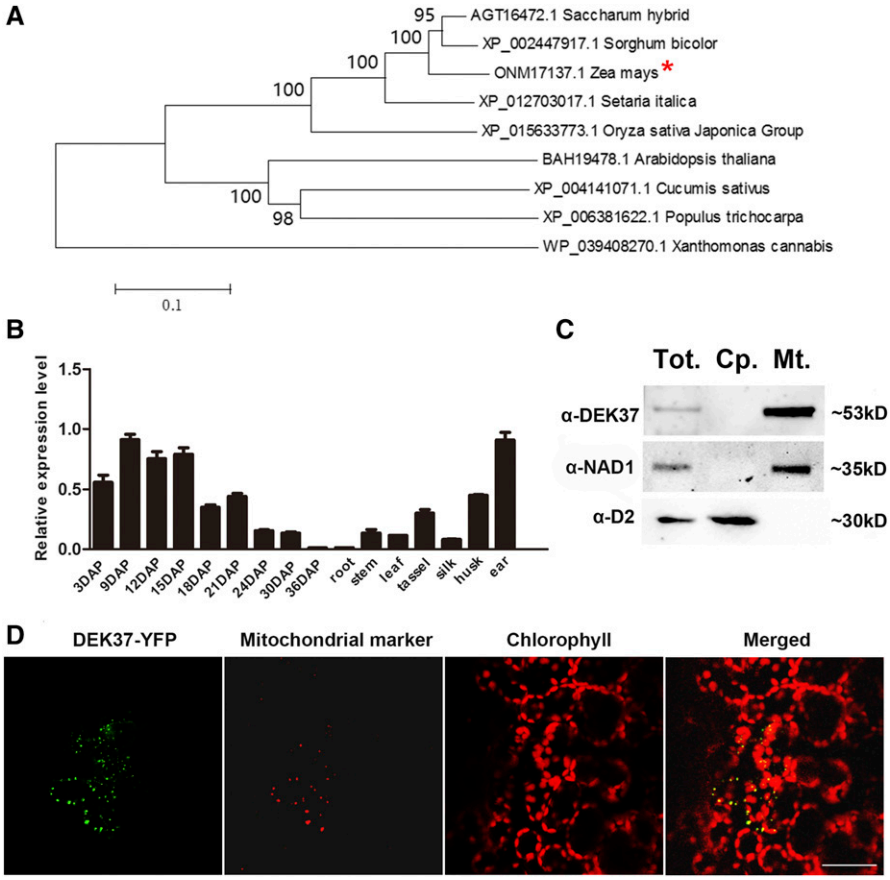

Figure 3 Phylogenetic analysis, expression pattern, and subcellular localization of DEK37. (A) Phylogenetic relationships of DEK37 and its homologs. The asterisk identifies ZmDEK37. (B) RNA expression level of *Dek37* in various tissues and expression profiles of *Dek37* during seed development. Ubiquitin was used as an internal control. Representative results from three biological replicates are shown. For each RNA sample, three technical replicates were performed. Values are means with SE; $n = 3$ individuals. (C) Immunoblot analysis of total (Tot.), chloroplastic (Cp.), and mitochondrial (Mt.) protein preparations with antibodies against DEK37, NAD1 (mitochondrial marker), and D2 (chloroplastic marker). Each lane was loaded with ~25 μg of protein preparation. (D) Subcellular localization in tobacco leaf epidermal cells. DEK37-YFP represents the YFP fusion protein at the C-terminus of full-length DEK37 protein. The mitochondrial signals are marked by mitochondria-mCherry marker. The chloroplast signals are autofluorescence. Bar, 10 μm.

expression level of *matR*, a maturase gene encoded by *nad1* intron 4 (Wahleithner *et al.* 1990), was increased in *dek37* (Figure 4A and Figure S6 in File S1). This was further confirmed by quantitative RT-PCR (Figure S7 in File S1).

The *nad2* gene, which encodes subunit 2 of complex I, is fragmented into five coding segments in the maize mitochondrial genome (Clifton *et al.* 2004). One *trans*-splicing event and three *cis*-splicing events are necessary for the complete maturation of the *nad2* transcript (Figure 4B). To further examine the splicing of *nad2* precursor transcript, we designed four specific primers to amplify fragments containing each of the four introns of *nad2* transcript in both *dek37*-ref and *dek37*-mu. In both *dek37*-ref and *dek37*-mu, the *cis*-spliced fragment of *nad2* mRNA joining exon 1/exon 2 was clearly attenuated and the unspliced fragment signal containing *nad2* intron 1 was clearly stronger than that in the WT, whereas the three other introns of *nad2* were correctly and efficiently spliced (Figure 4C).

To further investigate the splicing alterations in *dek37*, specific primers were designed for quantitative RT-PCR to inspect 22 mitochondrial group II introns in both *dek37*-ref and *dek37*-mu. The quantitative differences in spliced and unspliced fragments between WT and *dek37* mutants were compared with amplifying primers across adjacent exons and across adjacent exons and introns, respectively. The results showed significant reduction of the *nad2* spliced exon 1-2 fragment (Figure 5A) and increase of the *nad2* unspliced intron 1 fragment (Figure 5B) in both *dek37* mutants as compared with the WT. Dramatic reduction of splicing efficiency of *nad2* intron 1 was observed in both *dek37* mutants as indicated by the ratio of mature transcripts to unspliced fragments (Figure 5C). All these results indicated that the splicing efficiency of *nad2* intron 1 was decreased in *dek37* mutants and suggested that *Dek37* participates in the *cis*-splicing of mitochondrial *nad2* intron 1. Interestingly, a slight reduction in splicing efficiency and mature transcripts of *nad1* intron 4 were also observed in *dek37* mutants (Figure 5, A and C).

PPR proteins may recognize RNA sequences via a one PPR motif-one nucleotide module, and the amino acids at particular positions (6 and 1') in each repeat determine the nucleotide-binding specificity (Barkan *et al.* 2012; Miranda *et al.* 2017). We predicted the DEK37 PPR binding sites in *nad2* intron 1 according to a combinatorial amino acid code for RNA recognition by PPR proteins (Barkan *et al.* 2012; Miranda *et al.* 2017). Three candidate RNA sequences that DEK37 PPR might bind in *nad2* intron 1 were identified (Figure S8 in File S1). Further experiments are required to test if the DEK37 PPR protein can really bind to these candidate sequences.

The dek37 mutation affects mitochondrial complex I assembly and NADH dehydrogenase activity

The NAD2 protein is a central anchor component of complex I and would be expected to be essential for assembly of complex I in the membrane. Thus, blue native polyacrylamide gel

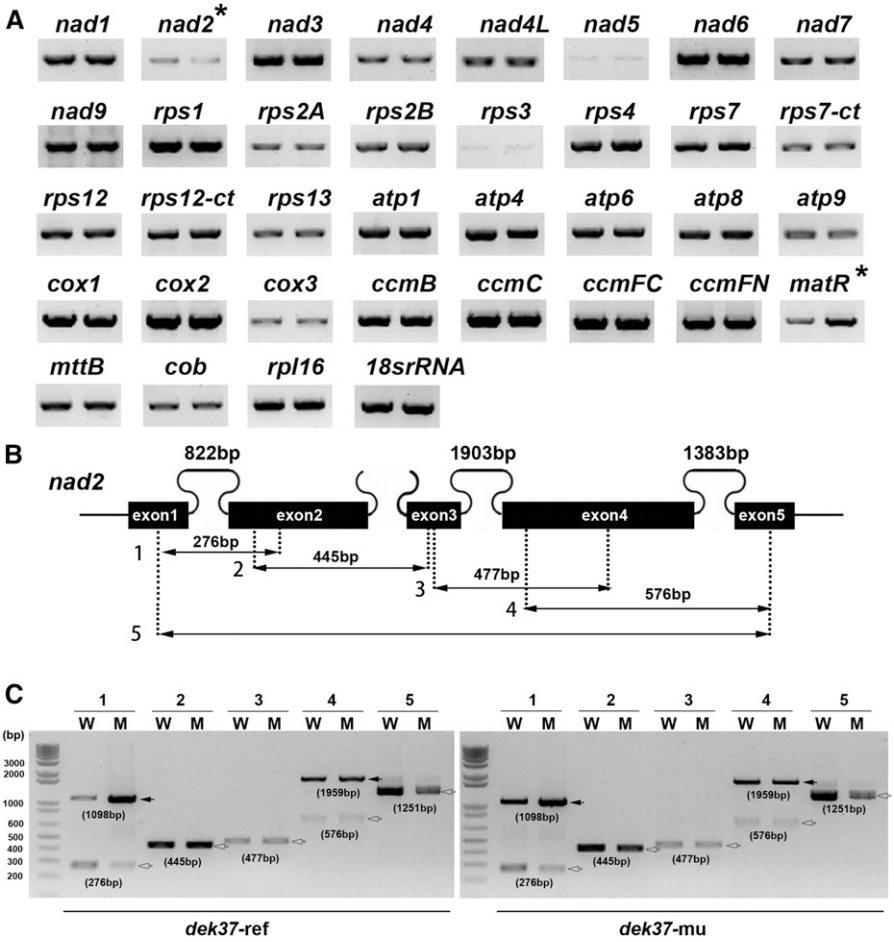

Figure 4 The decrease of *nad2* mature transcript and the splicing deficiency of *nad2* intron 1 in *dek37*. (A) RT-PCR analysis of 35 mitochondria-encoded transcripts in WT (left) and *dek37* (right) seeds. The RNA was isolated from the same ear segregating for WT and *dek37* seeds at 18 DAP. *18s rRNA* served as internal control. The asterisks identify *nad2* with decreased transcript abundance, and *matR* with increased transcript abundance. (B) Structure of the maize mitochondrial *nad2* gene. Intron 1, 3, and 4 are *cis*-spliced introns. Intron 2 is a *trans*-spliced intron. The expected amplification products using different primer pairs are indicated. (C) RT-PCR analysis of *nad2* intron-splicing efficiency in WT and *dek37* mutants. The solid and hollow arrows correspond to unspliced and spliced fragments, respectively. The expected sizes of amplification products using different primer pairs are indicated below each band. W, WT; M, mutant.

electrophoresis (BN-PAGE) was carried out to detect the potential impact on mitochondrial complexes in *dek37*-ref seeds. The mitochondria were isolated from WT and *dek37*-ref immature seeds at 18 DAP, and the purified mitochondria were separated through BN-PAGE. Complex I was found to be reduced in *dek37*-ref as compared with the WT (Figure 6A). An in-gel NADH dehydrogenase activity test was further carried out to inspect the activity of complex I. The results showed reduced NADH dehydrogenase activities of complex I and super complex I+III_2 in *dek37*-ref (Figure 6B). These results indicated that the assembly and NADH dehydrogenase activity of complex I were affected in *dek37*-ref seeds.

To further detect the impact of *dek37* mutation on the respiration chain complexes, mitochondrial complex-related proteins were analyzed by western blot with specific antibodies against NAD1 (subunit of complex I), CytC (cytochrome c), and COX2 (subunit of complex IV). The α-tubulin was used as a loading control. A dramatic decrease in NAD1 was detected while CytC was slightly increased in *dek37*-ref. The level of COX2 in *dek37*-ref was higher than that in the WT seeds (Figure 6C). These results suggested that the *dek37* mutation affected the assembly of complex I, which probably in return changed the accumulation of other complex-related proteins in *dek37*-ref.

The dek37 mutation causes abnormal mitochondrial morphology

To detect the impacts of *dek37* mutation in mitochondrial structure, WT and *dek37* endosperms at 18 DAP were observed by transmission electron microscopy (TEM). In *dek37*, mitochondria were observed to have severe deformations and voided internal structures. There were less typical cristae and lighter mitochondrial matrix in *dek37* compared with the WT. Furthermore, the whole structure of mitochondria was dilated and irregular in *dek37* (Figure 6E). These results indicated severe morphological changes of mitochondria in *dek37*. Along with the developmental delay of endosperm cells, it suggested that proper mitochondrial functions are required for maize seed development.

The dek37 mutation affects the expression of mitochondrial function-related genes

To better understand the impacts of *dek37* mutation on seed gene expression, RNA sequencing (RNA-seq) was used to compare the transcript profiles in WT and *dek37* endosperm from immature seeds at 18 DAP. Among all the 63,236 gene transcripts detected by RNA-seq, significant DEGs were identified as those with a threshold fold change >2 and $P < 0.01$. Based on this criterion, 1370 genes showed significantly altered expression between WT and *dek37*. There were 1105

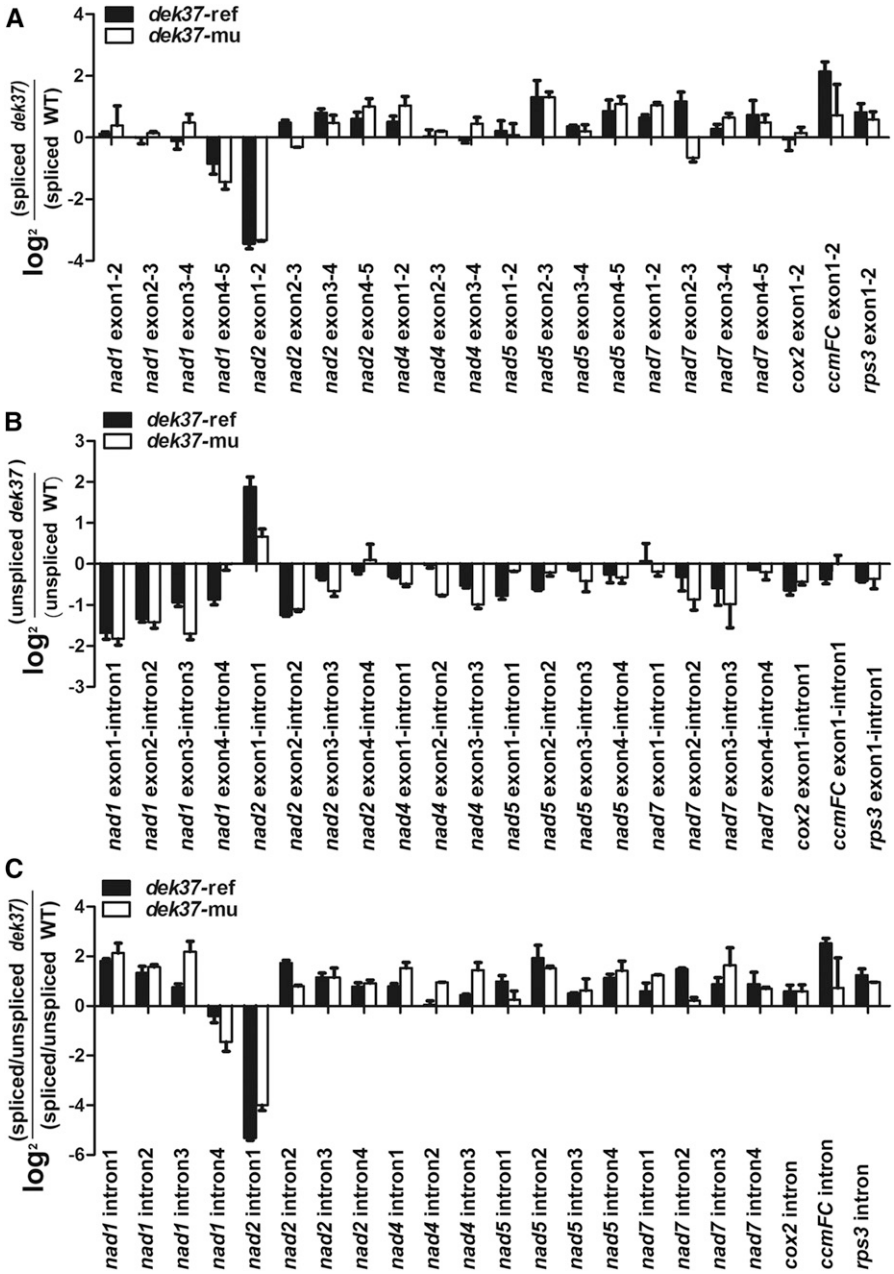

Figure 5 The *dek37* mutation affects *cis*-splicing of mitochondrial *nad2* intron1. Ubiquitin was used as an internal control. Representative results from three biological replicates are shown. Values are the means with SE; $n = 3$ individuals. (A) Quantitative RT-PCR analysis of mature transcripts. Primers spanning adjacent exons were used for measuring differences in each spliced fragment. (B) Quantitative RT-PCR analysis of unspliced fragments. Primers spanning adjacent exons and introns were used for measuring differences in each unspliced fragment. (C) Quantitative RT-PCR analysis of splicing efficiency of mitochondrial introns. The ratio of mature transcripts to unspliced fragments was used for measuring differences in splicing efficiency.

genes with increased transcription, while 265 genes showed decreased transcription (Table S1 in File S1).

Among 1370 DEGs, 932 genes could be functionally annotated (BLAST against GenBank database at http://www.ncbi.nlm.nih.gov). Using the Gene Ontology (GO) database (http://bioinfo.cau.edu.cn/agriGO), we found the most significant GO classifications of DEGs were associated with the primary mitochondrial function (Figure 6F). DEGs related to mitochondrial envelope (GO: 0005740, *P* value = 3.01E−07) that played important roles in mitochondrial activities exhibited extensively up-regulated transcriptional expression, indicating the function of mitochondria was greatly affected in the *dek37*. In addition, monosaccharide metabolic process (GO: 0005996, *P* value = 4.54E−05), translation (GO: 0006412, *P* value = 1.94E−02), cellular amino acid metabolic process (GO: 0006520, *P* value = 1.34E−05), tricarboxylic acid cycle (GO: 0006099, *P* value = 1.02E−03), and ion transport (GO: 0006811, *P* value = 0.00821) were also observed to be up-regulated, suggesting dramatic effects on the oxidation respiratory chain in *dek37*. Meanwhile, DEGs related to nucleosome assembly (GO: 0006334, *P* value = 7.63E−31) also exhibited significant up-regulation. On the other hand, DEGs related to nutrient reservoir activity (GO: 0045735, *P* value = 6.54E−28), which were mainly storage proteins, were down-regulated. This is in accordance with reduced total protein content in *dek37* mature seeds (Figure S1, A and B in File S1).

The previously described maize mutants lacking complex I had elevated levels of alternative oxidase (*Aox*) (Xiu *et al.* 2016; Chen *et al.* 2017; Qi *et al.* 2017b). The alternative

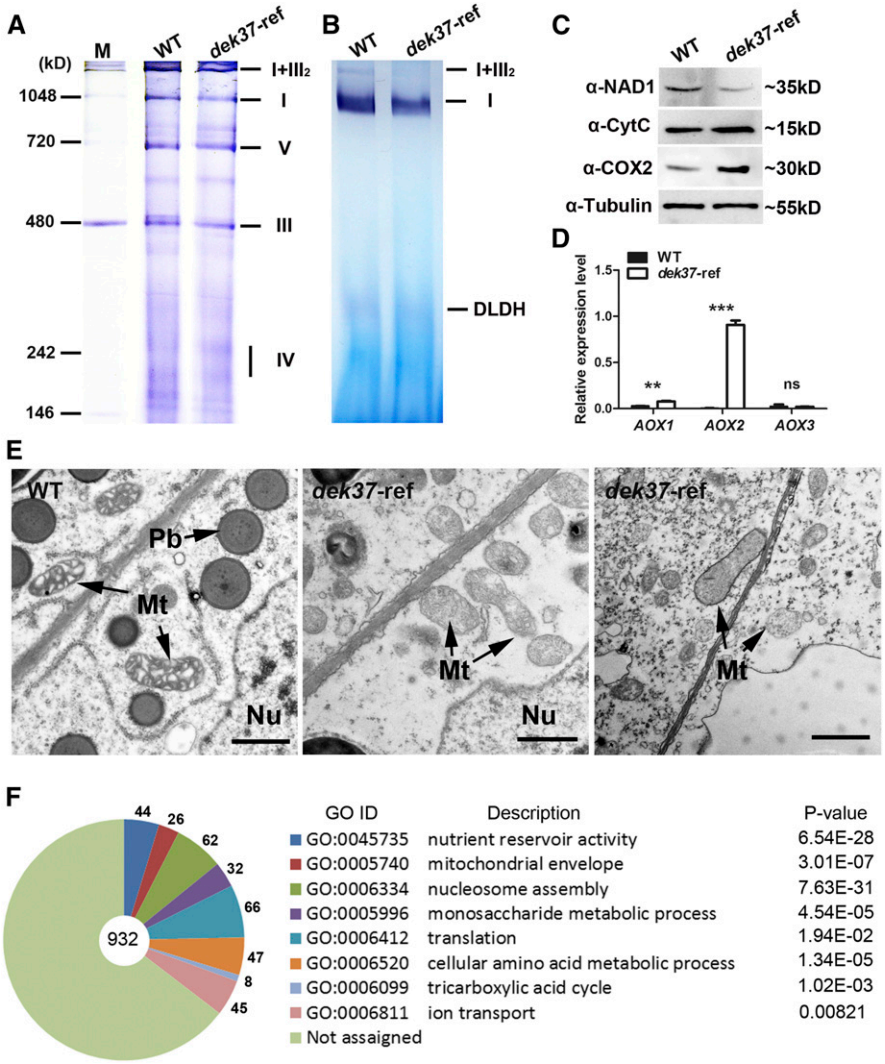

Figure 6 Affected mitochondrial function in *dek37* mutant seeds. (A) BN-PAGE analysis of mitochondrial complexes. The positions of super complex I+III$_2$, complex I, complex III, complex IV, and complex V were indicated. Each lane was loaded with ~250 μg of mitochondrial protein. I, III, IV, and V, complexes I, II, III, IV, and V; I+III$_2$, super complex composed of complex I and dimeric complex III. (B) In-gel NADH dehydrogenase activity test of complex I. The positions of complex I and super complex I+III$_2$ were indicated. The activity of the dehydrolipoamide dehydrogenase (DLDH) was used as a sample loading control. Each lane was loaded with ~250 μg of mitochondrial protein. (C) Western blot comparing accumulation of complex-related proteins NAD1 (subunit of complex I), CytC (cytochrome c), and COX2 (subunit of complex IV) in total seed protein from WT and *dek37*-ref immature seeds at 18 DAP. α-tubulin was used as a sample loading control. (D) Quantitative RT-PCR analysis of genes associated with the alternative respiratory pathway including *Aox1*, *Aox2*, and *Aox3*. Ubiquitin served as internal control. Values are the means with SE; $n = 3$ individuals (ns, not significant; ** $P < 0.01$, *** $P < 0.001$, Student's *t*-test). (E) Ultrastructure of developing endosperms from WT and *dek37*-ref seeds (18 DAP) for mitochondria observation. Bar, 1 μm. Mt, mitochondrion; Pb, protein body. (F) The most significantly related GO terms of the 932 functional annotated DEGs. The significance and number of genes classified within each GO term are shown.

pathway was examined by analyzing the expression levels of alternative oxidase (*Aox*) genes in *dek37*. The maize genome contains three *Aox* genes, *Aox1* (AY059646.1), *Aox2* (AY059647.1), and *Aox3* (AY059648.1). Quantitative RT-PCR revealed that the transcription level of *Aox2* was substantially increased in the *dek37* compared with WT (Figure 6D). RNA-seq data were further validated by quantitative RT-PCR on some of the most significant DEGs from each GO category (Figure S9 in File S1). The results were in accordance with RNA-seq data.

Discussion

Dek37 encodes a newly characterized P-type PPR protein that participates in cis-splicing of mitochondrial nad2 intron 1 in maize

Our results clearly showed that DEK37 is a classic P-type PPR protein that participates in *cis*-splicing of mitochondrial *nad2* intron 1 in maize. The functional characterization of DEK37 enlarges the list of P-type PPR proteins acting in organelle RNA metabolism as a splicing factor (Schmitz-Linneweber *et al.* 2006; de Longevialle *et al.* 2007; Beick *et al.* 2008; Keren *et al.* 2009, 2012; Koprivova *et al.* 2010; Liu *et al.* 2010; Khrouchtchova *et al.* 2012; Cohen *et al.* 2014; Colas des Francs-Small *et al.* 2014; Hsieh *et al.* 2015; Xiu *et al.* 2016; Cai *et al.* 2017; Chen *et al.* 2017; Qi *et al.* 2017b). The P-type PPR proteins with splicing effects have mainly been studied in *Arabidopsis* mitochondria, including OTP43 (de Longevialle *et al.* 2007), ABO5 (Liu *et al.* 2010), OTP439 and TANG2 (Colas des Francs-Small *et al.* 2014), SLO3 (Hsieh *et al.* 2015), and three nuclear Mat (nMat) genes (Keren *et al.* 2009, 2012; Cohen *et al.* 2014). In maize, PPR4 is associated *in vivo* with *trans*-splicing intron 1 of the plastid *rps12* transcript (Schmitz-Linneweber *et al.* 2006). PPR5 is another PPR protein that is bound to the *trnG*-UCC precursor in maize chloroplasts (Beick *et al.* 2008). THA8 is a short P-type PPR protein associated with splicing of introns in chloroplast *ycf3-2* and *trnA* (Khrouchtchova *et al.* 2012). EMP16 is specifically required for *cis*-splicing of *nad2* intron 4 in maize mitochondria (Xiu *et al.* 2016). EMP10 affects *cis*-splicing of *nad2* intron 1 and seed development in maize (Cai *et al.* 2017). DEK35 affects *cis*-splicing of mitochondrial *nad4* intron 1 in maize (Chen *et al.* 2017). DEK2 is involved

in mitochondrial *nad1* mRNA splicing in maize (Qi *et al.* 2017b).

Both a decrease in mature transcript and an increase in the unspliced form of *nad2* intron 1 were detected as compared with the WT, indicating the splicing efficiency of the *nad2* intron 1 was affected in *dek37* mutants (Figure 5). In comparison, all other introns in the mutant mitochondria were correctly spliced to a large extent in *dek37* mutants (Figure 5). Slight reductive splicing efficiency and mature transcript of *nad1* intron 4 were also observed in *dek37*. However, we did not find an increase in the unspliced form in *nad1* intron 4 (Figure 5), which indicated that *nad1* intron 4 might not be the direct splicing target of DEK37. This could be due to the effects from the increased expression of mitochondrial transcript *matR* or pleiotropic effects of the loss of complex I in maize seeds. Further analysis of mitochondrial complexes showed reduced assembly and NADH dehydrogenase activity of complex I (Figure 6), suggesting defects occurred in mitochondrial function in *dek37* as a consequence of a deficient *nad2* transcript.

The splicing of bacterial and yeast mitochondrial group II introns is facilitated by proteins encoded within the introns (*i.e.*, maturases), which act specifically in splicing of their host introns (Schmitz-Linneweber *et al.* 2015). In *Brassicaceae* mitochondria, MatR is required for splicing of *nad1* intron4. Knockdown of *matR* by synthetic *trans*-cleaving hammerhead ribozymes resulted in reduced mRNA level in *nad1* intron4 (Sultan *et al.* 2016). We noticed that expression of *matR* transcript was higher in *dek37* (Figure 4). This may reflect the discrepancies in the reduced splicing efficiency of *nad1* intron 4 in *dek37*. Similarly, elevated levels of many mitochondrial mRNAs were also seen in *otp43*, *nmat1*, and *nmat4* mutants (de Longevialle *et al.* 2007; Keren *et al.* 2012; Cohen *et al.* 2014), which are also affected in the maturation of *nad1* and show reduced complex I levels. The mechanisms by which altered expression of particular mitochondrial RNAs influence global mitochondrial gene expression or RNA metabolism are currently under investigation.

The splicing of many plastidic introns in maize involves multiple nuclear-encoded RNA-binding cofactors (Barkan 2011). In *dek37*, the splicing of *nad2* intron 1 was not completely abolished, indicating that although DEK37 functions in the splicing of *nad2* intron 1, the protein is not essential for maturation of *nad2* transcript, and suggesting the involvement of additional organellar factors. The defective splicing of *nad2* intron 1 was also observed in the *emp10* mutant (Cai *et al.* 2017), which suggests other factors involved in the splicing of *nad2* intron 1 in maize.

The dek37 mutation affects complex I assembly, mitochondrial function, seed development, and seedling growth in maize

Complex I is embedded in the inner membrane and mediates transfer of electrons from NADH to ubiquinone (Lee *et al.* 2013). Previous studies demonstrated the splicing defects are expected to influence the assembly and/or stability of complex I (de Longevialle *et al.* 2007; Keren *et al.* 2012; Cohen *et al.* 2014; Chen *et al.* 2017; Qi *et al.* 2017b). Several studies indicated that complex I was compromised in *dek37*. BN-PAGE and in-gel NADH dehydrogenase activity analysis revealed that the assembly and activity of complex I were reduced in *dek37* (Figure 6). Further Western blot using antibody against NAD1 (subunit of complex I) showed a large reduction in *dek37* (Figure 6). In *dek37*, no significant differences of complex III, IV, and V were observed in BN-PAGE as compared with the WT. However, CytC (cytochrome c), which is located in the mitochondrial intermembrane/ intercristae spaces and functions as an electron shuttle in the respiratory chain and interacts with cardiolipin (Garrido *et al.* 2006), showed slight increase in *dek37*. Similar to EMP16 (Xiu *et al.* 2016), increased COX2 (subunit of complex IV) level was also observed in *dek37*. Therefore, the *dek37* mutation affects the assembly and NADH dehydrogenase activity of complex I, which probably in return stimulates the accumulation of other complex-related proteins in *dek37*.

Complex I is the primary entry point for electrons into the electron transport chain, inhibition of which by inhibitors or by loss of subunits leads to problems with primary metabolism in the affected plants (Noctor *et al.* 2007). Previous studies showed that the alternative respiratory pathway is engaged under these conditions (Sabar *et al.* 2000; Karpova *et al.* 2002; de Longevialle *et al.* 2007; Sosso *et al.* 2012; Xiu *et al.* 2016; Chen *et al.* 2017; Qi *et al.* 2017b). Our data also shows that the alternative respiratory response is significantly induced in this mutant, with a significant transcriptional increase of alternative oxidase (*Aox*) genes (Figure 6). Furthermore, TEM indicated voided internal structures with abnormal mitochondrial morphology in *dek37* (Figure 6). Similar mitochondrial morphology observed in *dek35* (Chen *et al.* 2017) and *dek2* (Qi *et al.* 2017b) has been previously found to be associated with mitochondrial biogenesis defects in maize, suggesting that mitochondrial function was severely disordered in *dek37*.

Mitochondria are the central coordinators of energy metabolism, and alterations in their function and number have been associated with metabolic disorders such as diabetes and hyper-lipidemias. Among eight GO classifications, five GO classifications that were highly related to mitochondrial structure and activity exhibited extensive up-regulated DEGs, which indicated that the oxidation respiratory chain was severely affected in *dek37* (Figure 6). In *dek37*, voided internal structures and abnormal mitochondrial morphology were shown by TEM (Figure 6), suggesting its critical effects on mitochondrial function, which is in accordance with the increased mitochondrial envelope (GO: 0005740) in transcriptome analysis. In monosaccharide metabolic processes (GO: 0005996), energy obtained from oxidation of glucose is usually stored temporarily within cells in the form of ATP in mitochondria (Jenkins *et al.* 1984). The tricarboxylic acid cycle (GO: 0006099) (TCA cycle) is a series of enzyme-catalyzed chemical reactions that form a key part of aerobic respiration in mitochondria. Ion transport (GO: 0006811) across cellular

membranes is important for cellular homeostasis and has integrative functions such as transepithelial transport or neuronal signal transduction, which consumes energy produced by mitochondria (Lehninger 1970). Cellular amino acid metabolic processes (GO: 0006520) also need the energy from mitochondrial activity. In addition, nucleosome assembly (GO: 0006334) and translation (GO: 0006412) also exhibited significant up-regulation. Nucleosome assembly and translation are essential for seed development (Qi *et al.* 2016). The *dek37* mutation causes abnormal mitochondrial function, which results in feedback up-regulation of nucleosome assembly and translation-related genes for developmental delay (Figure 1 and Figure S1 in File S1). Apart from seven up-regulated GO classifications, only one GO classification (nutrient reservoir activity, GO: 0045735) showed decreased DEGs (Table S1 in File S1). Proper mitochondrial activity is essential for general protein synthesis (Rébeillé *et al.* 2007; Birke *et al.* 2012). The mature *dek37* seeds exhibited significantly reduced seed dry weight and protein contents as a result of defective mitochondrial function (Figure 1 and Figure S1 in File S1). Therefore, it was naturally expected that this transcriptional regulation resulted from the primary defect of energy production in mitochondria.

In *dek37*, inhibited development of BETL leads to delayed seed development that was further demonstrated by phenotype analysis of mature seeds. BETL was considered to play a central role in nutrient distribution (Royo *et al.* 2007). Previous studies have indicated that reduced BETL cells lead to delayed seed development (Xiu *et al.* 2016; Chen *et al.* 2017; Qi *et al.* 2017b). During normal endosperm development, cells in the BETL develop highly specialized cell wall ingrowths that increase the surface area of the associated plasmalemma to facilitate the uptake of nutrients from the maternal sporophyte to the seed (Thompson *et al.* 2001). These cells contain dense cytoplasm rich in mitochondria and organelles of the endomembrane secretory system located close to the wall invaginations (Davis *et al.* 1990). Thus, the arrested BETL development in *dek37* might be the consequence of reduced energy for nutrient transporting. In addition, the reduced energy caused by impaired mitochondrial function resulted in defective embryos, leading to a low level of germination rate and seedling lethality in *dek37*. Hence, the *dek37* mutation affects seed development and seedling growth due to abnormal mitochondrial function.

Acknowledgments

This work was supported by the National Key Research and Development Program of China (2016YFD0101003) and the National Natural Sciences Foundation of China (91635303, 31425019, and 31401386). There is no conflict of interest.

Author contributions: RS designed the experiment. DD, SL, XC, QW, and YF performed the experiments. DD, WQ, and RS analyzed the data. DD, WQ, and RS wrote the article.

Literature Cited

Aubourg, S., N. Boudet, M. Kreis, and A. Lecharny, 2000 In Arabidopsis thaliana, 1% of the genome codes for a novel protein family unique to plants. Plant Mol. Biol. 42: 603–613.

Barkan, A., 2011 Expression of plastid genes: organelle-specific elaborations on a prokaryotic scaffold. Plant Physiol. 155: 1520–1532.

Barkan, A., M. Rojas, S. Fujii, A. Yap, Y. S. Chong *et al.*, 2012 A combinatorial amino acid code for RNA recognition by pentatricopeptide repeat proteins. PLoS Genet. 8: e1002910.

Beick, S., C. Schmitz-Linneweber, R. Williams-Carrier, B. Jensen, and A. Barkan, 2008 The pentatricopeptide repeat protein PPR5 stabilizes a specific tRNA precursor in maize chloroplasts. Mol. Cell. Biol. 28: 5337–5347.

Birke, H., S. J. Muller, M. Rother, A. D. Zimmer, S. N. Hoernstein *et al.*, 2012 The relevance of compartmentation for cysteine synthesis in phototrophic organisms. Protoplasma 249(Suppl. 2): S147–S155.

Bonen, L., and J. Vogel, 2001 The ins and outs of group II introns. Trends Genet. 17: 322–331.

Brandt, U., 2006 Energy converting NADH:quinone oxidoreductase (complex I). Annu. Rev. Biochem. 75: 69–92.

Cai, M., S. Li, F. Sun, Q. Sun, H. Zhao *et al.*, 2017 Emp10 encodes a mitochondrial PPR protein that affects the cis-splicing of nad2 intron 1 and seed development in maize. Plant J. 91: 132–144.

Chen, X., F. Feng, W. Qi, L. Xu, D. Yao *et al.*, 2017 Dek35 encodes a PPR protein that affects cis-splicing of mitochondrial nad4 intron 1 and seed development in maize. Mol. Plant 10: 427–441.

Chomyn, A., M. W. Cleeter, C. I. Ragan, M. Riley, R. F. Doolittle *et al.*, 1986 URF6, last unidentified reading frame of human mtDNA, codes for an NADH dehydrogenase subunit. Science 234: 614–618.

Clayton, D. A., and G. S. Shadel, 2014 Purification of mitochondria by sucrose step density gradient centrifugation. Cold Spring Harb. Protoc. 2014: pdb.prot080028.

Clifton, S. W., P. Minx, C. M. Fauron, M. Gibson, J. O. Allen *et al.*, 2004 Sequence and comparative analysis of the maize NB mitochondrial genome. Plant Physiol. 136: 3486–3503.

Coffin, J. W., R. Dhillon, R. G. Ritzel, and F. E. Nargang, 1997 The Neurospora crassa cya-5 nuclear gene encodes a protein with a region of homology to the Saccharomyces cerevisiae PET309 protein and is required in a post-transcriptional step for the expression of the mitochondrially encoded COXI protein. Curr. Genet. 32: 273–280.

Cohen, S., M. Zmudjak, C. Colas des Francs-Small, S. Malik, F. Shaya *et al.*, 2014 nMAT4, a maturase factor required for nad1 pre-mRNA processing and maturation, is essential for holocomplex I biogenesis in Arabidopsis mitochondria. Plant J. 78: 253–268.

Colas des Francs-Small, C., A. Falcon de Longevialle, Y. Li, E. Lowe, S. K. Tanz *et al.*, 2014 The pentatricopeptide repeat proteins TANG2 and ORGANELLE TRANSCRIPT PROCESSING439 are involved in the splicing of the multipartite nad5 transcript encoding a subunit of mitochondrial complex I. Plant Physiol. 165: 1409–1416.

Colcombet, J., M. Lopez-Obando, L. Heurtevin, C. Bernard, K. Martin *et al.*, 2013 Systematic study of subcellular localization of Arabidopsis PPR proteins confirms a massive targeting to organelles. RNA Biol. 10: 1557–1575.

Davis, R. W., J. D. Smith, and B. G. Cobb, 1990 A light and electron microscope investigation of the transfer cell region of maize caryopses. Can. J. Bot. 68: 471–479.

Delannoy, E., W. A. Stanley, C. S. Bond, and I. D. Small, 2007 Pentatricopeptide repeat (PPR) proteins as sequence-specificity factors in post-transcriptional processes in organelles. Biochem. Soc. Trans. 35: 1643–1647.

de Longevialle, A. F., E. H. Meyer, C. Andres, N. L. Taylor, C. Lurin *et al.*, 2007 The pentatricopeptide repeat gene OTP43 is required for trans-splicing of the mitochondrial nad1 Intron 1 in Arabidopsis thaliana. Plant Cell 19: 3256–3265.

Feng, L., J. Zhu, G. Wang, Y. Tang, H. Chen *et al.*, 2009 Expressional profiling study revealed unique expressional patterns and dramatic expressional divergence of maize alpha-zein super gene family. Plant Mol. Biol. 69: 649–659.

Fisk, D. G., M. B. Walker, and A. Barkan, 1999 Molecular cloning of the maize gene crp1 reveals similarity between regulators of mitochondrial and chloroplast gene expression. EMBO J. 18: 2621–2630.

Fromm, S., J. Senkler, H. Eubel, C. Peterhansel, and H. P. Braun, 2016 Life without complex I: proteome analyses of an Arabidopsis mutant lacking the mitochondrial NADH dehydrogenase complex. J. Exp. Bot. 67: 3079–3093.

Garrido, C., L. Galluzzi, M. Brunet, P. E. Puig, C. Didelot *et al.*, 2006 Mechanisms of cytochrome c release from mitochondria. Cell Death Differ. 13: 1423–1433.

Handa, H., 2003 The complete nucleotide sequence and RNA editing content of the mitochondrial genome of rapeseed (Brassica napus L.): comparative analysis of the mitochondrial genomes of rapeseed and Arabidopsis thaliana. Nucleic Acids Res. 31: 5907–5916.

Hashimoto, M., T. Endo, G. Peltier, M. Tasaka, and T. Shikanai, 2003 A nucleus-encoded factor, CRR2, is essential for the expression of chloroplast ndhB in Arabidopsis. Plant J. 36: 541–549.

Heazlewood, J. L., K. A. Howell, and A. H. Millar, 2003 Mitochondrial complex I from Arabidopsis and rice: orthologs of mammalian and fungal components coupled with plant-specific subunits. Biochim. Biophys. Acta 1604: 159–169.

Hsieh, W. Y., J. C. Liao, C. Y. Chang, T. Harrison, and C. Boucher, 2015 The SLOW GROWTH3 pentatricopeptide repeat protein is required for the splicing of mitochondrial NADH dehydrogenase subunit7 intron 2 in Arabidopsis. Plant Physiol. 168: 490–501.

Jenkins, D. J., T. M. Wolever, A. L. Jenkins, R. G. Josse, and G. S. Wong, 1984 The glycaemic response to carbohydrate foods. Lancet 2: 388–391.

Karpova, O. V., E. V. Kuzmin, T. E. Elthon, and K. J. Newton, 2002 Differential expression of alternative oxidase genes in maize mitochondrial mutants. Plant Cell 14: 3271–3284.

Keren, I., A. Bezawork-Geleta, M. Kolton, I. Maayan, E. Belausov *et al.*, 2009 AtnMat2, a nuclear-encoded maturase required for splicing of group-II introns in Arabidopsis mitochondria. RNA 15: 2299–2311.

Keren, I., L. Tal, C. C. des Francs-Small, W. L. Araujo, S. Shevtsov *et al.*, 2012 nMAT1, a nuclear-encoded maturase involved in the trans-splicing of nad1 intron 1, is essential for mitochondrial complex I assembly and function. Plant J. 71: 413–426.

Khrouchtchova, A., R. A. Monde, and A. Barkan, 2012 A short PPR protein required for the splicing of specific group II introns in angiosperm chloroplasts. RNA 18: 1197–1209.

Koprivova, A., C. C. des Francs-Small, G. Calder, S. T. Mugford, S. Tanz *et al.*, 2010 Identification of a pentatricopeptide repeat protein implicated in splicing of intron 1 of mitochondrial nad7 transcripts. J. Biol. Chem. 285: 32192–32199.

Kotera, E., M. Tasaka, and T. Shikanai, 2005 A pentatricopeptide repeat protein is essential for RNA editing in chloroplasts. Nature 433: 326–330.

Kubo, T., S. Nishizawa, A. Sugawara, N. Itchoda, A. Estiati *et al.*, 2000 The complete nucleotide sequence of the mitochondrial genome of sugar beet (Beta vulgaris L.) reveals a novel gene for tRNA(Cys)(GCA). Nucleic Acids Res. 28: 2571–2576.

Langmead, B., C. Trapnell, M. Pop, and S. L. Salzberg, 2009 Ultrafast and memory-efficient alignment of short DNA sequences to the human genome. Genome Biol. 10: R25.

Lee, C. P., N. L. Taylor, and A. H. Millar, 2013 Recent advances in the composition and heterogeneity of the Arabidopsis mitochondrial proteome. Front. Plant Sci. 4: 4.

Lehninger, A. L., 1970 Mitochondria and calcium ion transport. Biochem. J. 119: 129–138.

Li-Pook-Than, J., and L. Bonen, 2006 Multiple physical forms of excised group II intron RNAs in wheat mitochondria. Nucleic Acids Res. 34: 2782–2790.

Liu, Y., J. He, Z. Chen, X. Ren, X. Hong *et al.*, 2010 ABA overly-sensitive 5 (ABO5), encoding a pentatricopeptide repeat protein required for cis-splicing of mitochondrial nad2 intron 3, is involved in the abscisic acid response in Arabidopsis. Plant J. 63: 749–765.

Liu, Y. J., Z. H. Xiu, R. Meeley, and B. C. Tan, 2013 Empty pericarp5 encodes a pentatricopeptide repeat protein that is required for mitochondrial RNA editing and seed development in maize. Plant Cell 25: 868–883.

Lurin, C., C. Andres, S. Aubourg, M. Bellaoui, F. Bitton *et al.*, 2004 Genome-wide analysis of Arabidopsis pentatricopeptide repeat proteins reveals their essential role in organelle biogenesis. Plant Cell 16: 2089–2103.

Malek, O., and V. Knoop, 1998 Trans-splicing group II introns in plant mitochondria: the complete set of cis-arranged homologs in ferns, fern allies, and a hornwort. RNA 4: 1599–1609.

Meyer, E. H., T. Tomaz, A. J. Carroll, G. Estavillo, E. Delannoy *et al.*, 2009 Remodeled respiration in ndufs4 with low phosphorylation efficiency suppresses Arabidopsis germination and growth and alters control of metabolism at night. Plant Physiol. 151: 603–619.

Miranda, R. G., M. Rojas, M. P. Montgomery, K. P. Gribbin, and A. Barkan, 2017 RNA-binding specificity landscape of the pentatricopeptide repeat protein PPR10. RNA 23: 586–599.

Nelson, B. K., X. Cai, and A. Nebenführ, 2007 A multicolored set of in vivo organelle markers for co-localization studies in Arabidopsis and other plants. Plant J. 51: 1126–1136.

Noctor, G., R. De Paepe, and C. H. Foyer, 2007 Mitochondrial redox biology and homeostasis in plants. Trends Plant Sci. 12: 125–134.

Notsu, Y., S. Masood, T. Nishikawa, N. Kubo, G. Akiduki *et al.*, 2002 The complete sequence of the rice (Oryza sativa L.) mitochondrial genome: frequent DNA sequence acquisition and loss during the evolution of flowering plants. Mol. Genet. Genomics 268: 434–445.

Ostheimer, G. J., H. Hadjivassiliou, D. P. Kloer, A. Barkan, and B. W. Matthews, 2005 Structural analysis of the group II intron splicing factor CRS2 yields insights into its protein and RNA interaction surfaces. J. Mol. Biol. 345: 51–68.

Ostheimer, G. J., M. Rojas, H. Hadjivassiliou, and A. Barkan, 2006 Formation of the CRS2–CAF2 group II intron splicing complex is mediated by a 22-amino acid motif in the COOH-terminal region of CAF2. J. Biol. Chem. 281: 4732–4738.

Qi, W., J. Zhu, Q. Wu, Q. Wang, X. Li *et al.*, 2016 Maize reas1 mutant stimulates ribosome use efficiency and triggers distinct transcriptional and translational responses. Plant Physiol. 170: 971–988.

Qi, W., Z. Tian, L. Lu, X. Chen, X. Chen *et al.*, 2017a Editing of mitochondrial transcripts nad3 and cox2 by Dek10 is essential for mitochondrial function and maize plant development. Genetics 205: 1489–1501.

Qi, W., Y. Yang, X. Feng, M. Zhang, and R. Song, 2017b Mitochondrial function and maize kernel development requires Dek2, a pentatricopeptide repeat protein involved in nad1 mRNA splicing. Genetics 205: 239–249.

Rébeillé, F., C. Alban, J. Bourguignon, S. Ravanel, and R. Douce, 2007 The role of plant mitochondria in the biosynthesis of coenzymes. Photosynth. Res. 92: 149–162.

Royo, J., E. Gómez, and G. Hueros, 2007 Transfer cells, pp. 73–89 in *Plant Cell Monographs—Endosperm,* Vol. 8, edited by O.-A. Olsen. Springer, Berlin.

Sabar, M., R. De Paepe, and Y. de Kouchkovsky, 2000 Complex I impairment, respiratory compensations, and photosynthetic decrease in nuclear and mitochondrial male sterile mutants of Nicotiana sylvestris. Plant Physiol. 124: 1239–1250.

Schertl, P., and H. P. Braun, 2014 Respiratory electron transfer pathways in plant mitochondria. Front. Plant Sci. 5: 163.

Schmitz-Linneweber, C., R. E. Williams-Carrier, P. M. Williams-Voelker, T. S. Kroeger, A. Vichas *et al.*, 2006 A pentatricopeptide repeat protein facilitates the trans-splicing of the maize chloroplast rps12 pre-mRNA. Plant Cell 18: 2650–2663.

Schmitz-Linneweber, C., M. K. Lampe, L. D. Sultan, and O. Ostersetzer-Biran, 2015 Organellar maturases: a window into the evolution of the spliceosome. Biochim. Biophys. Acta 1847: 798–808.

Senkler, J., M. Senkler, H. Eubel, T. Hildebrandt, C. Lengwenus *et al.*, 2017 The mitochondrial complexome of Arabidopsis thaliana. Plant J. 89: 1079–1092.

Small, I. D., and N. Peeters, 2000 The PPR motif – a TPR-related motif prevalent in plant organellar proteins. Trends Biochem. Sci. 25: 46–47.

Sosso, D., S. Mbelo, V. Vernoud, G. Gendrot, A. Dedieu *et al.*, 2012 PPR2263, a DYW-subgroup pentatricopeptide repeat protein, is required for mitochondrial nad5 and cob transcript editing, mitochondrion biogenesis, and maize growth. Plant Cell 24: 676–691.

Sugiyama, Y., Y. Watase, M. Nagase, N. Makita, S. Yagura *et al.*, 2005 The complete nucleotide sequence and multipartite organization of the tobacco mitochondrial genome: comparative analysis of mitochondrial genomes in higher plants. Mol. Genet. Genomics 272: 603–615.

Sultan, L. D., D. Mileshina, F. Grewe, K. Rolle, S. Abudraham *et al.*, 2016 The reverse transcriptase/RNA maturase protein MatR is required for the splicing of various group II introns in Brassicaceae mitochondria. Plant Cell 28: 2805–2829.

Sun, F., X. Wang, G. Bonnard, Y. Shen, Z. Xiu *et al.*, 2015 Empty pericarp7 encodes a mitochondrial E-subgroup pentatricopeptide repeat protein that is required for ccmFN editing, mitochondrial function and seed development in maize. Plant J. 84: 283–295.

Thompson, R. D., G. Hueros, H. Becker, and M. Maitz, 2001 Development and functions of seed transfer cells. Plant Sci. 160: 775–783.

Till, B., C. Schmitz-Linneweber, R. Williams-Carrier, and A. Barkan, 2001 CRS1 is a novel group II intron splicing factor that was derived from a domain of ancient origin. RNA 7: 1227–1238.

Unseld, M., J. R. Marienfeld, P. Brandt, and A. Brennicke, 1997 The mitochondrial genome of Arabidopsis thaliana contains 57 genes in 366,924 nucleotides. Nat. Genet. 15: 57–61.

Uyttewaal, M., N. Arnal, M. Quadrado, A. Martin-Canadell, N. Vrielynck *et al.*, 2008 Characterization of Raphanus sativus pentatricopeptide repeat proteins encoded by the fertility restorer locus for Ogura cytoplasmic male sterility. Plant Cell 20: 3331–3345.

Wahleithner, J. A., J. L. MacFarlane, and D. R. Wolstenholme, 1990 A sequence encoding a maturase-related protein in a group II intron of a plant mitochondrial nad1 gene. Proc. Natl. Acad. Sci. USA 87: 548–552.

Williams-Carrier, R., N. Stiffler, S. Belcher, T. Kroeger, D. B. Stern *et al.*, 2010 Use of Illumina sequencing to identify transposon insertions underlying mutant phenotypes in high-copy Mutator lines of maize. Plant J. 63: 167–177.

Xiu, Z., F. Sun, Y. Shen, X. Zhang, R. Jiang *et al.*, 2016 EMPTY PERICARP16 is required for mitochondrial nad2 intron 4 cis-splicing, complex I assembly and seed development in maize. Plant J. 85: 507–519.

Communicating editor: J. Birchler